

Linear-response theory of spin Seebeck effect in ferromagnetic insulators

Hiroto Adachi,^{1,2,*} Jun-ichiro Ohe,^{1,2} Saburo Takahashi,^{3,2,1} and Sadamichi Maekawa^{1,2}

¹ *Advanced Science Research Center, Japan Atomic Energy Agency, Tokai 319-1195, Japan*

² *CREST, Japan Science and Technology Agency, Sanbancho, Tokyo 102-0075, Japan*

³ *Institute for Materials Research, Tohoku University, Sendai 980-8577, Japan*

(Dated: October 2, 2018)

We formulate a linear response theory of the spin Seebeck effect, i.e., a spin voltage generation from heat current flowing in a ferromagnet. Our approach focuses on the collective magnetic excitation of spins, i.e., magnons. We show that the linear-response formulation provides us with a qualitative as well as quantitative understanding of the spin Seebeck effect observed in a prototypical magnet, yttrium iron garnet.

I. INTRODUCTION

The generation of spin voltage, i.e., the potential for an electron's spin to drive spin currents, by a temperature gradient in a ferromagnet is referred to as the spin Seebeck effect (SSE). Since the first observation of the SSE in a ferromagnetic metal $\text{Ni}_{81}\text{Fe}_{19}$,¹ this phenomenon has attracted much attention as a new method of generating spin currents from heat energy and opened a new possibility of spintronics devices.² The SSE triggered the emergence of the new field dubbed “spin caloritronics”^{3,4} in the rapidly growing spintronics community. Moreover, as the induced spin voltage can be converted into electric voltage through the inverse spin Hall effect⁵ at the attached nonmagnetic metal, this phenomenon put a new twist on the long and well-studied history of thermoelectric research.⁶

One of the canonical frameworks to describe nonequilibrium transport phenomena is linear-response theory.⁷ Having been applied to a number of transport phenomena, linear-response theory has been so successful because it is intimately related to the universal fluctuation-dissipation theorem. Up to now, however, the linear-response formulation of the SSE has not been known mainly because, unlike the charge current, the spin current is not a conserved quantity. Therefore, it is of great importance to formulate the SSE in terms of linear-response theory.

Concerning the SSE, a big mystery is now being established, which is, how can conduction electrons sustain the spin voltage over such a long range of several millimeters¹ in spite of the conduction electrons' short spin-flip diffusion length, which is typically of several tens of nanometers? A key to resolve this puzzle was reported by a recent experiment on electric signal transmission through a ferromagnetic insulator⁸ which demonstrates that the spin current can be carried by the low-lying magnetic excitation of *localized* spins, i.e., the magnon excitations, and that it can transmit the spin current as far as several millimeters. Subsequently, the SSE was reported to be observed in the magnetic insulator $\text{LaY}_2\text{Fe}_5\text{O}_{12}$ despite the absence of conduction electrons.⁹ These experiments suggest that contrary to the conventional wisdom over the last two decades that the spin current is carried by

conduction electrons,¹⁰ the magnon is a promising candidate as a carrier for the SSE.

The purpose of this paper is twofold. First, we analyze the SSE observed in $\text{LaY}_2\text{Fe}_5\text{O}_{12}$ ⁹ (hereafter referred to as YIG) in terms of magnon spin current, i.e., a spin current carried by magnon excitations. Second, we develop a framework for analyzing the SSE by means of the standard linear-response formalism⁷ which is amenable to the language of the magnetism community.¹¹ This allows us to describe the spin transport phenomena systematically, and it can be easily generalized to a situation including degrees of freedom other than magnons, e.g., conduction electrons and phonons, to describe a more complicated process in the case of metallic systems.¹

The plan of this paper is as follows. In Sec. II, we present a linear-response approach to the “local” spin injection by thermal magnons, in which the spin injection is driven by the temperature difference between the ferromagnet and the attached nonmagnetic metal. Next, in Sec. III we develop a linear-response theory of the “non-local” spin injection by thermal magnons, in which the spin injection is driven by the temperature gradient inside the ferromagnet. As one can see below, this process can explain the SSE observed in YIG.⁹ Finally, in Sec. IV we summarize and discuss our results.

II. “LOCAL” SPIN INJECTION BY THERMAL MAGNONS

We start by briefly reviewing the SSE experiment for YIG.⁹ Figure 1 shows the experimental setup where several Pt terminals are attached on top of a YIG film in a static magnetic field $H_0\hat{z}$ (\gg anisotropy field) which aligns the localized magnetic moment along \hat{z} . A temperature gradient ∇T is applied along the z axis, and it induces a spin voltage across the YIG/Pt interface. This spin voltage then injects a spin current I_s into the Pt terminal (or ejects it from the Pt terminal). A part of the injected/ejected spin current I_s is converted into a charge voltage through the so-called inverse spin Hall effect.⁵

$$V_{\text{ISHE}} = \Theta_H(|e|I_s)(\rho/w), \quad (1)$$

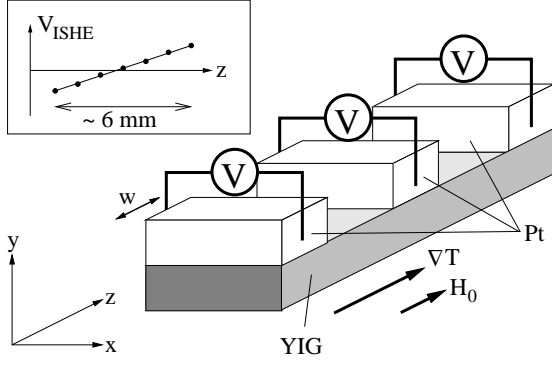


FIG. 1: Experimental setup for observing the SSE.⁹ Inset: Schematics of the spatial profile of the observed voltage.

where $|e|$, Θ_H , ρ , and w are the absolute value of electron charge, spin Hall angle, resistivity, and width of the Pt terminal (see Fig. 1), respectively. Hence, the observed charge voltage V_{ISHE} is a measure of the injected/ejected spin current I_s .

To investigate the SSE observed in YIG, we consider a model shown in Fig. 2(a). While YIG is a ferrimagnet, we model it as a ferromagnet since we are interested in the low-energy properties. The key point in our model is that the temperature gradient is applied over the insulating ferromagnet, but there is *locally* no temperature difference between the ferromagnet and the attached nonmagnetic metals, i.e., $T_{N_1} = T_{F_1} = T_1$, $T_{N_2} = T_{F_2} = T_2$, and $T_{N_3} = T_{F_3} = T_3$. We assume that each domain is initially in thermal equilibrium without interactions with the neighboring domains, and then calculate the nonequilibrium dynamics after we switch on the interactions. Note that this procedure is essentially equivalent to that used by Luttinger¹² to realize the initial condition mentioned above.

Let us consider first the low-energy excitations in the ferromagnet. In the following, we focus on the spin-wave region where the magnetization $\mathbf{M}(\mathbf{r})$ fluctuates only weakly around the ground state value $M_s \hat{z}$ with the saturation magnetization M_s , and we set $\mathbf{M}/M_s = (1 - m^2/2)\hat{z} + \mathbf{m}$ to separate the small fluctuation part \mathbf{m} ($\perp \hat{z}$) from the ground state value. Then, the low-energy excitations of \mathbf{M} are described by boson (magnon) operators $a_{\mathbf{q}}^\dagger$ and $a_{\mathbf{q}}$ through the relations¹³ $m_{\mathbf{q}}^\dagger = \sqrt{1/S_0} a_{-\mathbf{q}}^\dagger$ and $m_{\mathbf{q}}^- = \sqrt{1/S_0} a_{\mathbf{q}}$ where $m^\pm \equiv (m^x \pm im^y)/\sqrt{2}$, S_0 is the size of localized spins, and $\mathbf{m}(\mathbf{r}, t) = N_F^{-1/2} \sum_{\mathbf{q}} \mathbf{m}_{\mathbf{q}}(t) e^{i\mathbf{q}\cdot\mathbf{r}}$ with N_F being the number of localized spins in the ferromagnet. Consistent with this boson mapping, the magnetization dynamics is described by the following action:^{14,15}

$$\mathcal{S}_F = \int_C dt \sum_{\mathbf{q}} m_{-\mathbf{q}}^\dagger(t) [X_{\mathbf{q}}(i\partial_t)]^{-1} m_{\mathbf{q}}^-(t), \quad (2)$$

where the integration is performed along the Keldysh contour C ,¹⁶ and the bare magnon propagator is given

by

$$\check{X}_{\mathbf{q}}(\omega) = \begin{pmatrix} X_{\mathbf{q}}^R(\omega), & X_{\mathbf{q}}^K(\omega) \\ 0, & X_{\mathbf{q}}^A(\omega) \end{pmatrix} \quad (3)$$

with the following equilibrium condition:

$$X_{\mathbf{q}}^A(\omega) = [X_{\mathbf{q}}^R(\omega)]^*, \quad X_{\mathbf{q}}^K(\omega) = 2i \text{Im} X_{\mathbf{q}}^R(\omega) \coth\left(\frac{\hbar\omega}{2k_B T}\right)$$

The retarded component of $\check{X}_{\mathbf{q}}(\omega)$ is given by $X_{\mathbf{q}}^R(\omega) = S_0^{-1}(\omega - \tilde{\omega}_{\mathbf{q}} + i\alpha\omega)^{-1}$ where α is the Gilbert damping constant, and $\tilde{\omega}_{\mathbf{q}} = \gamma H_0 + \omega_{\mathbf{q}}$ is the magnon frequency. Here, γ is the gyromagnetic ratio and $\omega_{\mathbf{q}} = D_{\text{ex}} q^2$, where $D_{\text{ex}} = 2S_0 J_{\text{ex}} a_S^2$ is the spin-wave stiffness constant with J_{ex} and a_S^3 being the exchange energy and the effective block spin volume.

In the nonmagnetic metal, the dynamics of the spin density \mathbf{s} can be described by the action¹⁷

$$\mathcal{S}_N = \int_C dt \sum_{\mathbf{k}} s_{-\mathbf{k}}^+(t) [\chi_{\mathbf{k}}(i\partial_t)]^{-1} s_{\mathbf{k}}^-(t), \quad (5)$$

where $s_{\mathbf{k}}^\pm = (s_{\mathbf{k}}^x \pm is_{\mathbf{k}}^y)/2$ is defined by $\mathbf{s}_{\mathbf{k}} = N_N^{-1/2} \sum_{\mathbf{p}} c_{\mathbf{p}+\mathbf{k}}^\dagger \boldsymbol{\sigma} c_{\mathbf{p}}$ with $\boldsymbol{\sigma}$, $c_{\mathbf{p}}^\dagger = (c_{\mathbf{p},\uparrow}^\dagger, c_{\mathbf{p},\downarrow}^\dagger)$, and N_N being the Pauli matrices, the electron creation operator for spin projection \uparrow and \downarrow , and the number of atoms in the nonmagnetic metal. The equilibrium spin-density propagator is given by

$$\check{\chi}_{\mathbf{k}}(\omega) = \begin{pmatrix} \chi_{\mathbf{k}}^R(\omega), & \chi_{\mathbf{k}}^K(\omega) \\ 0, & \chi_{\mathbf{k}}^A(\omega) \end{pmatrix} \quad (6)$$

with the following equilibrium condition:

$$\chi_{\mathbf{k}}^A(\omega) = [\chi_{\mathbf{k}}^R(\omega)]^*, \quad \chi_{\mathbf{k}}^K(\omega) = 2i \text{Im} \chi_{\mathbf{k}}^R(\omega) \coth\left(\frac{\hbar\omega}{2k_B T}\right)$$

The retarded part of $\check{\chi}$ is given by¹⁸ $\chi_{\mathbf{k}}^R(\omega) = \chi_N (1 + \lambda_N^2 k^2 - i\omega\tau_{\text{sf}})^{-1}$ with χ_N , λ_N , and τ_{sf} being the paramagnetic susceptibility, spin diffusion length, and spin relaxation time, the form of which is consistent with the corresponding diffusive Bloch equation [see Eq. (10) below].

Finally, the interaction between magnons and spin density at the interface is given by

$$\mathcal{S}_{F-N} = \int_C dt \sum_{\mathbf{k}, \mathbf{q}} \frac{S_0 \mathcal{J}_{\text{sd}}^{k-q}}{\sqrt{N_F N_N}} \mathbf{m}_{-\mathbf{q}}(t) \cdot \mathbf{s}_{\mathbf{k}}(t), \quad (8)$$

where $\mathcal{J}_{\text{sd}}^{k-q}$ is the Fourier transform of $\mathcal{J}_{\text{sd}}(\mathbf{r}) = J_{\text{sd}} \xi_0(\mathbf{r})$ with J_{sd} being the s - d exchange interaction between conduction-electron spins and localized spins, and $\xi_0(\mathbf{r}) = \sum_{\mathbf{r}_0 \in \text{N-N interface}} a_S^3 \delta(\mathbf{r} - \mathbf{r}_0)$.

It is instructive to point out that in the spin-wave region and in the classical limit with negligible quantum fluctuations, a system described by Eqs. (2), (5), and (8) is equivalent^{15,19} to a system described by the stochastic Landau-Lifshitz-Gilbert equation,

$$\partial_t \mathbf{M} = [\gamma(\mathbf{H}_{\text{eff}} + \mathbf{h}) - \frac{\mathcal{J}_{\text{sd}}}{\hbar} \mathbf{s}] \times \mathbf{M} + \frac{\alpha}{M_s} \mathbf{M} \times \partial_t \mathbf{M} \quad (9)$$

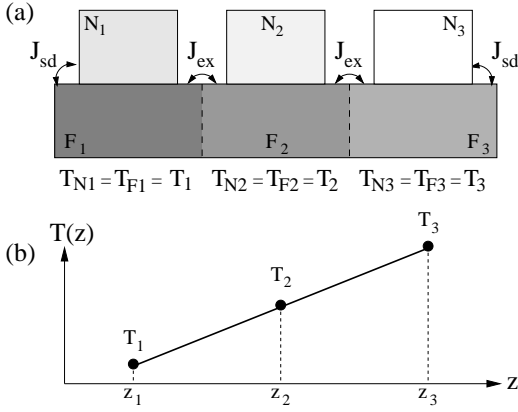


FIG. 2: (a) System composed of ferromagnet (F) and non-magnetic metals (N) divided into the three temperature domains of F_1/N_1 , F_2/N_2 , and F_3/N_3 with their local temperatures of T_1 , T_2 , and T_3 . (b) Temperature profile.

coupled with the Bloch equation,²⁰

$$\partial_t \mathbf{s} = (D_N \nabla^2 - \tau_{\text{sf}}^{-1}) \delta \mathbf{s} + \frac{J_{\text{sd}}}{\hbar M_s} \mathbf{M} \times \mathbf{s} + \mathbf{l}, \quad (10)$$

where $\mathbf{H}_{\text{eff}} = H_0 \hat{z} + (D_{\text{ex}}/\gamma) \nabla^2 (\mathbf{M}/M_s)$, $D_N = \lambda_N^2/\tau_{\text{sf}}$ is the diffusion constant, and $\delta \mathbf{s}(\mathbf{r}) = \mathbf{s}(\mathbf{r}) - s_0 \xi_0(\mathbf{r}) \mathbf{M}(\mathbf{r})/M_s$ is the spin accumulation with the local equilibrium spin density $s_0 = \chi_N S_0 J_{\text{sd}}/\hbar$. The noise field \mathbf{h} represents thermal fluctuations in F with $\langle h_i(\mathbf{r}, t) \rangle = 0$ and $\langle h_i(\mathbf{r}, t) h_j(\mathbf{r}', t') \rangle = \frac{2k_B T(\mathbf{r}) \alpha}{\gamma M_s} \delta_{ij} \delta(\mathbf{r} - \mathbf{r}') \delta(t - t')$,²¹ while the noise source \mathbf{l} in N satisfies $\langle l_i(\mathbf{r}, t) \rangle = 0$ and $\langle l_i(\mathbf{r}, t) l_j(\mathbf{r}', t') \rangle = \frac{2k_B T(\mathbf{r}) \chi_N a^3}{\tau_{\text{sf}}} \delta_{ij} \delta(\mathbf{r} - \mathbf{r}') \delta(t - t')$ ²² with the lattice constant a , both of which are postulated by the fluctuation-dissipation theorem.

In this section we focus on the “local” spin injection from F_1 into N_1 . The spin current induced in N_1 can be calculated from the linear response expression of the magnon-mediated spin injection given in the Appendix A [Eq. (A4)]. Consider the process P_1 shown in Fig. 3 (a) where magnons travel around the ferromagnet F_1 without feeling the temperature difference between F_1 and F_2 . Using the standard rules of constructing the Feynman diagram in Keldysh space,¹⁶ the corresponding interface Green’s function $\check{C}_{\mathbf{k}, \mathbf{q}}(\omega)$ for the correlation between the magnons in F_1 and the spin density in N_1 [Eq. (A4)] can be written in the form

$$\check{C}_{\mathbf{k}, \mathbf{q}}(\omega) = \frac{J_{\text{sd}}^{k-q} S_0}{\sqrt{N_N N_F}} \check{\chi}_{\mathbf{k}}(\omega) \check{X}_{\mathbf{q}}(\omega), \quad (11)$$

where N_N and N_F are the number of lattice sites in N_1 and F_1 . Substituting Eq. (11) into Eq. (A4) and employing the equilibrium conditions [Eqs. (4) and (7)], we obtain the expression for the injected spin current

$$I_s^{N_1} = -\frac{4N_{\text{int}} J_{\text{sd}}^2 S_0^2}{\sqrt{2} \hbar^2 N_N N_F} \sum_{\mathbf{q}, \mathbf{k}} \int_{\omega} \text{Im} \chi_{\mathbf{k}}^R(\omega) \text{Im} X_{\mathbf{q}}^R(\omega) \times \left[\coth\left(\frac{\hbar\omega}{2k_B T_{N_1}}\right) - \coth\left(\frac{\hbar\omega}{2k_B T_{F_1}}\right) \right], \quad (12)$$

where we have introduced the shorthand notation $\int_{\omega} = \int_{-\infty}^{\infty} \frac{d\omega}{2\pi}$, and N_{int} is the number of localized spins at the N_1 - F_1 interface playing a role of the number of channels. The ω integration can be performed by picking up only magnon poles under the condition $\alpha \hbar \tilde{\omega}_{\mathbf{q}} \ll k_B T_{N_1}, k_B T_{F_1}$ (always satisfied for YIG), giving $\int_{\omega} \text{Im} \chi_{\mathbf{k}}(\omega) \text{Im} X_{\mathbf{q}}(\omega) [\coth(\frac{\hbar\omega}{2k_B T})] \approx -\frac{1}{2} \text{Im} \chi_{\mathbf{k}}(\tilde{\omega}_{\mathbf{q}}) [\coth(\frac{\hbar\tilde{\omega}_{\mathbf{q}}}{2k_B T})]$. By making the classical approximation $\coth(\frac{\hbar\tilde{\omega}_{\mathbf{q}}}{2k_B T}) \approx \frac{2k_B T}{\hbar\tilde{\omega}_{\mathbf{q}}}$, we obtain

$$I_s^{N_1} = \frac{N_{\text{int}} J_{\text{sd}}^2 S_0 \chi_N \tau_{\text{sf}}}{2\sqrt{2} \pi^4 \hbar^3 (\lambda_N/a)^3} \Upsilon_1 k_B (T_{N_1} - T_{F_1}), \quad (13)$$

where $\Upsilon_1 = \int_0^1 dx \int_0^1 dy \frac{x^2 \sqrt{y}}{[(1+x^2)^2 + y^2 (2J_{\text{ex}} S_0 \tau_{\text{sf}}/\hbar)^2]}$ with the dimensionless variables $x = \mathbf{k} \lambda_N$ and $y = \hbar\omega_{\mathbf{q}}/(2J_{\text{ex}} S_0)$, and we used the relation $N_F^{-1} \sum_{\mathbf{q}} = (2\pi)^{-2} \int \sqrt{y} dy$.

III. MAGNON-MEDIATED SPIN SEEBECK EFFECT

Equation (13) means that, through the “local” process P_1 shown in Fig. 3(a), the spin current is *not* injected into the nonmagnetic metal N_1 when F_1 and N_1 have the same temperature. That is, the “local” process cannot explain the experiment⁹ where no temperature difference exists between the YIG film and the attached Pt film. A way to account for the experiment within the “local” picture is to invoke a difference between the phonon temperature and magnon temperature.²³ In this paper, on the other hand, we take a different route and consider the effect of temperature gradient *within* the YIG film on the spin injection into the Pt terminal.

The basic idea of our approach is as follows. The above result [Eq. (13)] that the injected spin current vanishes when $T_{F_1} = T_{N_1}$ originates from the equilibrium condition of the magnon propagator [Eq. (4)]. When magnons deviate from local thermal equilibrium by allowing the magnons to feel the temperature gradient inside the ferromagnet, the magnon propagator cannot be written in the equilibrium form, and it generates a nontrivial contribution to the thermal spin injection. The relevant “non-local” process P'_1 is shown in Fig. 3(a) in which magnons feel the temperature difference between F_1 and F_2 . The interaction between F_1 and F_2 is described by the action

$$S_{F-F} = \int_C dt \sum_{\mathbf{q}, \mathbf{q}'} \frac{2J_{\text{ex}}^{q-q'} S_0^2}{N_F} \mathbf{m}_{\mathbf{q}}(t) \cdot \mathbf{m}_{-\mathbf{q}'}(t), \quad (14)$$

where $J_{\text{ex}}^{q-q'}$ is the Fourier transform of $J_{\text{ex}}(\mathbf{r}) = J_{\text{ex}} \xi_1(\mathbf{r})$ with $\xi_1(\mathbf{r}) = \sum_{\mathbf{r}_0 \in F-F \text{ interface}} a_S^3 \delta(\mathbf{r} - \mathbf{r}_0)$.

We now regard the whole of the magnon lines appearing in the process P'_1 as a single magnon propagator $\delta \check{X}_{\mathbf{q}}(\omega)$, namely,

$$\delta \check{X}_{\mathbf{q}}(\omega) = \frac{1}{N_F^2} \sum_{\mathbf{q}'} |J_{\text{ex}}^{q-q'}|^2 \check{X}_{\mathbf{q}}(\omega) \check{X}_{\mathbf{q}'}(\omega) \check{X}_{\mathbf{q}}(\omega). \quad (15)$$

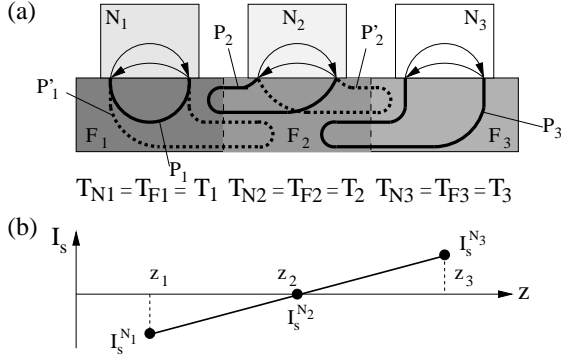


FIG. 3: (a) Feynman diagrams expressing the spin current injected from the ferromagnet (F) to the nonmagnetic metals (N). The thin solid lines with arrows (bold lines without arrows) represent electron propagators (magnon propagators). (b) Spatial profile of the calculated spin current.

Then the propagator is decomposed into the local-equilibrium part and nonequilibrium part as²⁴

$$\delta\tilde{X}_{\mathbf{q}}(\omega) = \delta\tilde{X}_{\mathbf{q}}^{l-eq}(\omega) + \delta\tilde{X}_{\mathbf{q}}^{n-eq}(\omega), \quad (16)$$

where

$$\delta\tilde{X}_{\mathbf{q}}^{l-eq} = \begin{pmatrix} \delta X_{\mathbf{q}}^{l-eq,R}, \delta X_{\mathbf{q}}^{l-eq,K} \\ 0, \delta X_{\mathbf{q}}^{l-eq,A} \end{pmatrix} \quad (17)$$

is the local-equilibrium propagator satisfying the local-equilibrium condition, i.e., $\delta X_{\mathbf{q}}^{l-eq,A} = [\delta X_{\mathbf{q}}^{l-eq,R}]^*$ and $\delta X_{\mathbf{q}}^{l-eq,K} = [\delta X_{\mathbf{q}}^{l-eq,R} - \delta X_{\mathbf{q}}^{l-eq,A}] \coth(\frac{\hbar\omega}{2k_B T})$ with

$$\delta X_{\mathbf{q}}^{l-eq,R}(\omega) = \frac{1}{N_F^2} \sum_{\mathbf{q}'} |\mathcal{J}_{\text{ex}}^{\mathbf{q}-\mathbf{q}'}|^2 (X_{\mathbf{q}}^R(\omega))^2 X_{\mathbf{q}'}^R(\omega), \quad (18)$$

while

$$\delta\tilde{X}_{\mathbf{q}}^{n-eq} = \begin{pmatrix} 0, \delta X_{\mathbf{q}}^{n-eq,K} \\ 0, 0 \end{pmatrix} \quad (19)$$

is the nonequilibrium propagator with $\delta X_{\mathbf{q}}^{n-eq,K}(\omega)$ given by

$$\begin{aligned} \delta X_{\mathbf{q}}^{n-eq,K}(\omega) &= \sum_{\mathbf{q}'} \frac{|2\mathcal{J}_{\text{ex}}^{\mathbf{q}-\mathbf{q}'} S_0|^2}{N_F^2} [X_{\mathbf{q}'}^R(\omega) - X_{\mathbf{q}'}^A(\omega)] \\ &\times |X_{\mathbf{q}}^R(\omega)|^2 \left[\coth\left(\frac{\hbar\omega}{2k_B T_{F_2}}\right) - \coth\left(\frac{\hbar\omega}{2k_B T_{F_1}}\right) \right] \end{aligned}$$

Note that the local equilibrium propagator [Eq. (17)] does not contribute to the “nonlocal” spin injection.

When we substitute Eq. (16) into Eq. (A4) and use Eq. (11) with $\tilde{X}_{\mathbf{q}}(\omega)$ being replaced by $\delta\tilde{X}_{\mathbf{q}}(\omega)$, we obtain the following expression for the magnon-mediated thermal spin injection:

$$\begin{aligned} I_s^{N_1} &= \frac{-4J_{\text{sd}}^2 S_0 (2J_{\text{ex}} S_0)^2 N_{\text{int}} N'_{\text{int}}}{\sqrt{2}\hbar^2 N_F^3 N_N} \sum_{\mathbf{q}, \mathbf{q}', \mathbf{k}} \int_{\omega} \text{Im}\chi_{\mathbf{k}}^R(\omega) \\ &\times |X_{\mathbf{q}}^R(\omega)|^2 \text{Im}X_{\mathbf{q}'}^R(\omega) \left[\coth\left(\frac{\hbar\omega}{2k_B T_1}\right) - \coth\left(\frac{\hbar\omega}{2k_B T_2}\right) \right], \end{aligned}$$

where N'_{int} is the number of localized spins at the F_1 - F_2 interface, and we used $T_{N_i} = T_{F_i} = T_i$ ($i = 1, 2$). The ω integration can be performed as before, giving $\int_{\omega} \text{Im}\chi_{\mathbf{k}}^R(\omega) |X_{\mathbf{q}}^R(\omega)|^2 \text{Im}X_{\mathbf{q}'}^R(\omega) \left[\coth\left(\frac{\hbar\omega}{2k_B T_1}\right) - \coth\left(\frac{\hbar\omega}{2k_B T_2}\right) \right] \approx \frac{-\pi}{2\alpha\tilde{\omega}_{\mathbf{q}}} \delta(\omega_{\mathbf{q}} - \omega_{\mathbf{q}'}') \text{Im}\chi_{\mathbf{k}}^R(\tilde{\omega}_{\mathbf{q}}) \left[\coth\left(\frac{\hbar\tilde{\omega}_{\mathbf{q}}}{2k_B T_1}\right) - \coth\left(\frac{\hbar\tilde{\omega}_{\mathbf{q}}}{2k_B T_2}\right) \right]$, which suggests that the magnon modes with different \mathbf{q} 's do not interfere with each other. With the classical approximation $\coth\left(\frac{\hbar\tilde{\omega}_{\mathbf{q}}}{2k_B T}\right) \approx \frac{2k_B T}{\hbar\tilde{\omega}_{\mathbf{q}}}$, we obtain

$$I_s^{N_1} = \frac{N_{\text{int}} (J_{\text{sd}}^2 S_0) \chi_N \tau_{\text{sf}} (a/\lambda_N)^3}{8\sqrt{2}\pi^5 \hbar^3 \alpha (\Lambda/a_S)} \Upsilon_2 k_B \delta T, \quad (22)$$

where $\delta T = T_1 - T_2$, Λ is the size of F_1 along the temperature gradient, and $\Upsilon_2 = \int_0^1 dx \int_0^1 dy \frac{y^2}{[(1+x^2)^2 + y^2 (2S_0 J_{\text{ex}} \tau_{\text{sf}}/\hbar)^2]}$ which is approximated as $\Upsilon_2 \approx 0.1426$ ($\Upsilon_2 \approx 0.337\hbar/2S_0 J_{\text{ex}} \tau_{\text{sf}}$) for $2S_0 J_{\text{ex}} \tau_{\text{sf}}/\hbar \lesssim 1$ (for $2S_0 J_{\text{ex}} \tau_{\text{sf}}/\hbar \gg 1$).

The spin current $I_s^{N_3}$ injected into the right terminal N_3 can be calculated in the same manner by considering the process P_3 , which gives $I_s^{N_3} = -I_s^{N_1}$ from the relation $T_1 - T_2 = -(T_3 - T_2)$. The spin current $I_s^{N_2}$ injected into the middle terminal N_2 vanishes because the two relevant processes (P_2 and P_2') cancel out. Therefore, we obtain the spatial profile of the injected spin current as shown in Fig. 3(b). Note that the effect of the spatial dependence of magnetization $\mathbf{M}[T(\mathbf{r})]$ through the local temperature $T(\mathbf{r})$ is already taken into account in our treatment because the temperature dependence of \mathbf{M} in the magnon region is automatically described by the number of thermal magnons discussed in this paper.

For an order of magnitude estimation, we compare Eq. (22) with the experiment.⁹ By using $\Theta_H \approx 0.0037$,^{25,26} $\rho = 15.6 \times 10^{-8} \Omega\text{m}$, $w = 0.1 \text{ mm}$, $\lambda_N \approx 7 \text{ nm}$, $\tau_{\text{sf}} \approx 1 \text{ ps}$, $a = 2 \text{ \AA}$, $a_S = 12.3 \text{ \AA}$, $S_0 = 16$, $\alpha \approx 5 \times 10^{-5}$,⁸ $\chi_N = 1 \times 10^{-6} \text{ cm}^3/\text{g}$,²⁷ and $N_{\text{int}} = 0.1 \times 4\text{mm}^2/a_S^2$, the s - d exchange coupling extracted from the previous ferromagnetic resonance experiment⁸ ($J_{\text{sd}} \approx 10 \text{ meV}$) can account for the spin Seebeck voltage $V_{\text{ISHE}}/\delta T \approx 0.1 \mu\text{V}/\text{K}$ observed at room temperature.

Finally, we comment on the issue of length scales associated with the SSE. In the original SSE experiment for a *metallic* ferromagnet,¹ the signal maintained over several millimeters was a big surprise because the spin diffusion length for that system is much shorter than a millimeter. Concerning the magnon-mediated SSE in an *insulating* magnet⁹ which we have discussed, it is of crucial importance to recognize that the length scale relevant to the SSE is related to magnon density fluctuations and is given by *longitudinal* fluctuations of magnons, while the magnon mean free path is related to magnon dephasing and is given by *transverse* fluctuations of magnons.²⁸ It was shown by Mori and Kawasaki³⁰ that these two length scales do not coincide with each other since they obey quite different dynamics, and it was demonstrated that in a certain situation the length scale of magnon density fluctuations (which is relevant to the SSE as well) is much

longer than the magnon mean free path [see Eq.(6.33) in Ref. 30 where the length scale of long-wavelength magnon density fluctuations is infinitely long].³¹ The notion of these two different length scales is the key to understanding the length scales observed in the SSE experiment in an insulating magnet.⁹

IV. CONCLUSION

We have developed a theory of the magnon-mediated spin Seebeck effect in terms of the canonical framework of describing transport phenomena, i.e., the linear-response theory, and shown that it provides us with a qualitative as well as quantitative understanding of the spin Seebeck effect observed in a prototypical magnet, yttrium iron garnet.⁹ Because the carriers of spin current in this scenario are magnons, we can obtain a bigger signal for a magnetic material with a lower magnon damping [see Eq. (22) where the injected spin current is inversely proportional to the Gilbert damping constant α]. An advantage of our linear-response formulation is that it can be easily generalized to a situation including degrees of freedom other than magnons, e.g., phonons and conduction electrons, to describe a more complicated process in the case of metallic¹ and semiconducting systems,³³ and a calculation taking account of the effect of nonequilibrium phonons will be reported in a future publication.³⁴ A numerical approach to the SSE is also developed in Ref. 35. We believe that the present approach stimulates further research on the spin Seebeck effect.

Acknowledgments

We are grateful to E. Saitoh, K. Uchida, G. E. W. Bauer, and J. Ieda for helpful discussions. This work was financially supported by a Grant-in-Aid for Scientific Research on Priority Areas (No. 19048009) and a Grant-in-Aid for Young Scientists (No. 22740210) from MEXT, Japan.

Appendix A: Linear-response expression of magnon-induced spin injection

The Gaussian action for conduction electrons in the nonmagnetic metal N_i ($i = 1, 2, 3$) is given by

$$S_N = \int_C dt \sum_{\mathbf{p}, \mathbf{p}'} c_{\mathbf{p}}^\dagger(t) \left\{ i\partial_t - \left(\epsilon_{\mathbf{p}} \delta_{\mathbf{p}, \mathbf{p}'} + U_{\mathbf{p}-\mathbf{p}'} [1 + i\eta_{so} \boldsymbol{\sigma} \cdot (\mathbf{p} \times \mathbf{p}')] \right) \right\} c_{\mathbf{p}'}(t), \quad (\text{A1})$$

where $c_{\mathbf{p}}^\dagger = (c_{\mathbf{p}, \uparrow}^\dagger, c_{\mathbf{p}, \downarrow}^\dagger)$ is the electron creation operator for spin projection \uparrow and \downarrow , $U_{\mathbf{p}-\mathbf{p}'}$ is the Fourier transform of the impurity potential $U_{\text{imp}} \sum_{\mathbf{r}_0 \in \text{impurities}} \delta(\mathbf{r} - \mathbf{r}_0)$, and η_{so} measures the strength of the spin-orbit interaction.³⁶

At the ferromagnet/nonmagnetic-metal interface, the magnetic interaction between conduction-electron spin density and localized spin is described by the s - d interaction [Eq. (8)]. The spin current induced in the nonmagnetic metal N_1 can be calculated as the rate of change of the spin accumulation in N_1 , i.e., $I_s^{N_1}(t) \equiv \sum_{\mathbf{r} \in N_1} \langle \partial_t s^z(\mathbf{r}, t) \rangle = \langle \partial_t \tilde{s}_{\mathbf{k}_0}^z(t) \rangle_{\mathbf{k}_0 \rightarrow \mathbf{0}}$, where $\langle \dots \rangle$ means the statistical average at a given time t , and $\tilde{s}_{\mathbf{k}} = \sqrt{N_N} \mathbf{s}_{\mathbf{k}}$ with \mathbf{s} being defined below Eq. (5).

The Heisenberg equation of motion for $\tilde{s}_{\mathbf{k}_0}^z$ gives

$$\begin{aligned} \partial_t \tilde{s}_{\mathbf{k}_0}^z &= \sum_{\mathbf{q}, \mathbf{k}} \frac{i\mathcal{J}_{sd}^{k-q} S_0}{\sqrt{2N_F N_N} \hbar} \left(m_{-\mathbf{q}}^+ [s_{\mathbf{k}}^-, s_{\mathbf{k}_0}^z] + m_{-\mathbf{q}}^- [s_{\mathbf{k}}^+, s_{\mathbf{k}_0}^z] \right) \\ &= i \sum_{\mathbf{q}, \mathbf{k}} \frac{2\mathcal{J}_{sd}^{k-q} S_0}{\sqrt{2N_F N_N} \hbar} \left(m_{-\mathbf{q}}^+ s_{\mathbf{k}+\mathbf{k}_0}^- - m_{-\mathbf{q}}^- s_{\mathbf{k}+\mathbf{k}_0}^+ \right), \end{aligned} \quad (\text{A2})$$

where we have used the relation $[\tilde{s}_{\mathbf{k}}^z, \tilde{s}_{\mathbf{k}'}^\pm] = \pm 2\tilde{s}_{\mathbf{k}+\mathbf{k}'}^\pm$, and neglected a small correction term arising from the spin-orbit interaction assuming that the spin-orbit interaction is weak enough at the neighborhoods of the interface. Then, the statistical average of the above quantity gives the following spin current:

$$I_s^{N_1}(t) = \sum_{\mathbf{q}, \mathbf{k}} \frac{-4\mathcal{J}_{sd}^{k-q} S_0}{\sqrt{2N_F N_N} \hbar} \text{Re} C_{\mathbf{k}, \mathbf{q}}^<(t, t), \quad (\text{A3})$$

where $C_{\mathbf{k}, \mathbf{q}}^<(t, t') = -i \langle m_{-\mathbf{q}}^+(t') s_{\mathbf{k}}^-(t) \rangle$ is the interface Green's function. In the steady state, the Green's function $C_{\mathbf{k}, \mathbf{q}}^<(t, t')$ depends only on the time difference $t - t'$ as $C_{\mathbf{k}, \mathbf{q}}^<(t - t') = \int_{-\infty}^{\infty} \frac{d\omega}{2\pi} C_{\mathbf{k}, \mathbf{q}}^<(\omega) e^{-i\omega(t-t')}$. Adopting the representation³⁷ $\check{C} = \begin{pmatrix} C^R, C^K \\ 0, C^A \end{pmatrix}$ and using $C^< = \frac{1}{2}[C^K - C^R + C^A]$, we finally obtain

$$I_s^{N_1} = \sum_{\mathbf{q}, \mathbf{k}} \frac{-2\mathcal{J}_{sd}^{k-q} S_0}{\sqrt{2N_F N_N} \hbar} \int_{-\infty}^{\infty} \frac{d\omega}{2\pi} \text{Re} C_{\mathbf{k}, \mathbf{q}}^K(\omega) \quad (\text{A4})$$

for the spin current $I_s^{N_1}$ in a steady state. As in the case of tunneling charge current driven by a voltage difference,³⁸ the spin current $I_s^{N_1}$ can be calculated systematically.

* hiroto.adachi@gmail.com

¹ K. Uchida, S. Takahashi, K. Harii, J. Ieda, W. Koshibae,

- K. Ando, S. Maekawa, and E. Saitoh, *Nature* **455**, 778 (2008).
- ² I. Žutić, J. Fabian, and S. D. Sarma, *Rev. Mod. Phys.* **76**, 323 (2004).
 - ³ *Spin Caloritronics*, edited by G. E. W. Bauer, A. H. MacDonald, and S. Maekawa, special issue of *Solid State Commun.*, **150**, 459 (2010).
 - ⁴ J. C. Slonczewski, *Phys. Rev. B* **82**, 054403 (2010).
 - ⁵ E. Saitoh, M. Ueda, H. Miyajima, and G. Tatara, *Appl. Phys. Lett.* **88**, 182509 (2006).
 - ⁶ F. J. Blatt, P. A. Schroeder, C. L. Foiles, and D. Greig, *Thermoelectric Power of Metals* (Plenum Press, New York, 1976).
 - ⁷ For example, G. Mahan, *Many-Particle Physics* (Kluwer Academic, New York, 1981).
 - ⁸ Y. Kajiwara, K. Harii, S. Takahashi, J. Ohe, K. Uchida, M. Mizuguchi, H. Umezawa, H. Kawai, K. Ando, K. Takanashi, S. Maekawa, and E. Saitoh, *Nature* **464**, 262 (2010).
 - ⁹ K. Uchida, J. Xiao, H. Adachi, J. Ohe, S. Takahashi, J. Ieda, T. Ota, Y. Kajiwara, H. Umezawa, H. Kawai, G. E. W. Bauer, S. Maekawa, and E. Saitoh, *Nature Mater.* **9**, 894 (2010).
 - ¹⁰ *Concepts in Spin Electronics*, ed. S. Maekawa (Oxford University Press, Oxford, U.K., 2006).
 - ¹¹ E. Šimánek and B. Heinrich, *Phys. Rev. B* **67**, 144418 (2003).
 - ¹² J. M. Luttinger, *Phys. Rev.* **135**, A1505 (1964).
 - ¹³ A. I. Akhiezer, V. G. Baryakhtar, and M. I. Kaganov, *Usp. Fiz. Nauk* **71**, 533 (1960) [*Sov. Phys. Usp.* **3**, 567 (1961)].
 - ¹⁴ S. Doniach and E. H. Sondheimer, *Green's Functions for Solid State Physicists* (Benjamin, New York, 1974).
 - ¹⁵ A. Schmid, *J. Low Temp. Phys.* **49**, 609 (1982).
 - ¹⁶ For a review, see, e.g., J. Rammer and H. Smith, *Rev. Mod. Phys.* **58**, 323 (1986).
 - ¹⁷ J. A. Hertz and M. A. Klenin, *Phys. Rev. B* **10**, 1084 (1974).
 - ¹⁸ P. Fulde and A. Luther, *Phys. Rev.* **175**, 337 (1968).
 - ¹⁹ C. De Dominicis, *Nuovo Cimento Lett.* **12**, 567 (1975).
 - ²⁰ S. Zhang and Z. Li, *Phys. Rev. Lett.* **93**, 127204 (2004).
 - ²¹ W. F. Brown, Jr., *Phys. Rev.* **130**, 1677 (1963).
 - ²² S. Ma and G. F. Mazenko, *Phys. Rev. B* **11**, 4077 (1975).
 - ²³ J. Xiao, G. E. W. Bauer, K. Uchida, E. Saitoh, and S. Maekawa, *Phys. Rev. B* **81**, 214418 (2010).
 - ²⁴ K. Michaeli and A. M. Finkel'stein, *Phys. Rev.* **80**, 115111 (2009).
 - ²⁵ T. Kimura, Y. Otani, T. Sato, S. Takahashi, and S. Maekawa, *Phys. Rev. Lett.* **98**, 156601 (2007).
 - ²⁶ O. Mosendz, J. E. Pearson, F. Y. Fradin, G. E. W. Bauer, S. D. Bader, and A. Hoffmann, *Phys. Rev. Lett.* **104**, 046601 (2010).
 - ²⁷ C. Kriessman and H. Callen, *Phys. Rev.* **94**, 837 (1954).
 - ²⁸ Note that our scenario does not rely on the long propagation length of dipole magnons (\sim several millimeters) observed in Ref. 29, since the magnons which we have discussed here are of exchange origin.
 - ²⁹ T. Schneider, A. A. Serga, B. Leven, B. Hillebrands, R. L. Stamps, and M. P. Kostylev, *Appl. Phys. Lett.* **92**, 022505 (2008).
 - ³⁰ H. Mori and K. Kawasaki, *Prog. Theor. Phys.* **27**, 529 (1962).
 - ³¹ An analogous situation occurs for conduction electrons in a disordered metal³² where the length scale associated with the long-wavelength density fluctuations of conduction electrons is infinite due to the charge conservation while that related to the dephasing of conduction electrons, i.e., the mean free path of conduction electrons, is as short as several nanometers.
 - ³² D. Vollhardt and P. Wölfle, *Phys. Rev. B* **22**, 4666 (1980).
 - ³³ C. M. Jaworski, J. Yang, S. Mack, D. D. Awschalom, J. P. Heremans, and R. C. Myers, *Nature Mater.* **9**, 898 (2010).
 - ³⁴ H. Adachi, K. Uchida, E. Saitoh, J. Ohe, S. Takahashi, and S. Maekawa, *Appl. Phys. Lett.* **97**, 252506 (2010).
 - ³⁵ J. Ohe, H. Adachi, S. Takahashi, and S. Maekawa, *Phys. Rev. B* **83**, 115118 (2011).
 - ³⁶ S. Takahashi and S. Maekawa, *J. Phys. Soc. Jpn* **77**, 031009 (2008).
 - ³⁷ A. I. Larkin and Yu. N. Ovchinnikov, *Zh. Eksp. Teor. Fiz.* **68**, 1915 [*Sov. Phys. JETP* **41**, 960 (1976)].
 - ³⁸ C. Caroli, R. Combescot, P. Nozieres, and D. Saint-James, *J. Phys. C: Solid State Phys.* **4**, 916 (1971).